

Electronic Supplementary Material (ESI) for Journal of Materials Chemistry B.
This journal is © The Royal Society of Chemistry 2014

Supplementary Information

Synthesis, characterization and anticancer activity in vitro of the biomolecule-based coordination complex nanotubes

Yue Wang, ^{a,b} *Chi Zhang*, ^a *Hongmei Li*, ^b *Guoxing Zhu*, ^a *Song-Song Bao*, ^a *Shiqiang Wei*, ^a *Li-Min Zheng*, ^a *Min Ren*, ^a and *Zheng Xu* ^{a*}

a State Key Laboratory of Coordination Chemistry, School of Chemistry and Chemical Engineering, Nanjing University, Nanjing, 210093, P.R. China.

b State Key Laboratory of Natural Medicines, School of Sciences, China Pharmaceutical University, Nanjing, 210009, P.R. China.

Corresponding Authors

E-mail: zhengxu@nju.edu.cn

XRD result

The XRD pattern of Ni-folate BMB-CCNTs indicates the non-crystalline nature of the nanotubes, and none characteristic diffraction peaks of Ni (0) was observed in the BMB-CCNTs sample (Fig. 1S).

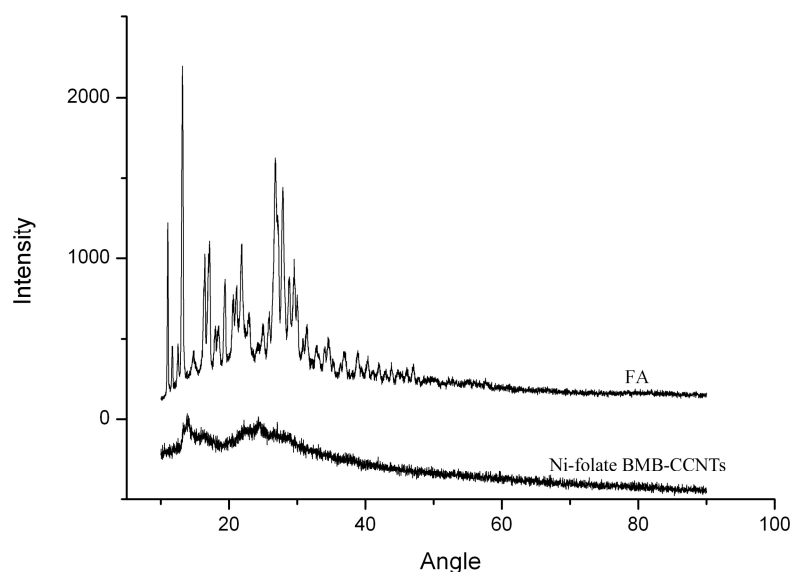


Fig. 1S XRD pattern of the Ni-folate BMB-CCNTs and FA

Absorption spectra

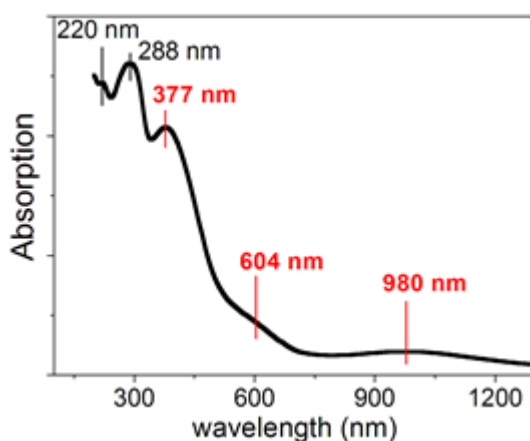


Fig. 2S UV-Vis-NIR spectra of Ni-folate BMB-CCNTs.

Infrared spectra data

The characteristic IR bands of the sample are summarized in Table 1S, and the bands of folic acid are shown for comparison. There is a very strong absorption band at 1694 cm^{-1} in the IR spectrum of folic acid; this band belongs to the stretching vibration of $\nu(\text{C}=\text{O})$ of the carboxylic group but disappears in the nanotube sample due to the chelating coordination. The bands at 1570 cm^{-1} and 1453 cm^{-1} in folic acid can be assigned to $\nu_{\text{as}}(\text{COO}^-)$ and $\nu_{\text{s}}(\text{COO}^-)$, respectively, while they shifted to 1537 cm^{-1} and 1401 cm^{-1} , respectively, in the Ni-folate BMB-CCNTs. Both the $\nu_{\text{as}}(\text{COO}^-)$ and $\nu_{\text{s}}(\text{COO}^-)$ bands shift in the same direction compared with free folic acid. The absorption bands of $\nu_{\text{as}}(\text{COO}^-)$ and $\nu_{\text{s}}(\text{COO}^-)$ in the

chelating or bridging coordination mode shift in the same direction, whereas the shift in the opposite direction in the case of monodentate coordination. Thus, bidentate coordination of COO⁻ to Ni ion was deduced for the CCNTs sample, in agreement with the XPS results.

Table 1S. Characteristic IR frequencies (cm⁻¹) of folic acid and the Ni-folate CCNTs

Assignments	Folic acid	Ni-folate BMB-sample
$\nu(\text{COOH})$	1694	-----
$\nu_{\text{as}}(\text{COO}^-)$	1565	1537
$\nu_{\text{s}}(\text{COO}^-)$	1453	1401
$\nu_{\text{s}}(\text{N-N})$	-----	983, 940

EXAFS measurements

The EXAFS measurements at the Ni-K edge (8333 eV) were carried out in transmission mode at the beamline U7C in the National Synchrotron Radiation Laboratory (NSRL) in China. In a typical experiment, about 41 mg of sample was ground into fine powder and mixed with ca. 116 mg of BN and then pressed into a 13.0 mm diameter circular sample holder. The spectrum of nickel foil was recorded periodically to check the energy calibration, and the first derivative of the nickel foil K-edge spectrum at 8333 eV was used to define the zero-energy reference point. The XANES spectra were background subtracted and were normalized to the edge step at the beginning of the EXAFS oscillations in order to make a meaningful comparison of the intensity of the pre-edge features. The EXAFS signals, $\chi(k)$, were extracted from the absorption raw data, $\mu(E)$, with ATHENA 0.8.056 program choosing the energy edge value (E_0) at the maximum derivative. The quantitative analysis was carried out with the IFEFFIT 1.2.11-ARTEMIS 0.8.012 program with the coordination sphere N₂O₄. Theoretical EXAFS signals were computed with the FEFF7.0 code using muffin-tin potentials and the Hedin-Lunqvist approximation for the energy-dependent part. The employed fitting ranges are summarized in Table 2S. The intrinsic reduction factor S_0^2 , the edge-energy shift ΔE_0 , the coordination number N, the inter-atomic distance R and the mean-square relative displacement σ^2 were fitted. The XANES spectra of two samples are given in Figure 4S. The Ni K-edge k³-weight (k) data and their Fourier-transformed (FT) data are shown in Figures 5S and 6S. The X-ray absorption near-edge structure (XANES) spectra further evidence above conjecture.

Table 2S. Forward Fourier Transform and backward Fourier Transform selected parameters of the Ni-N/O first shell at Ni-K edge.

Sample	Shell	K-range	Window type	R-range	Window type
Ni-FA	Ni-O	2.399~12.161	kaiser-bessel	1.044~1.993	kaiser-bessel
CCNTs	Ni-N/O	2.483~12.161	kaiser-bessel	1.040~1.993	kaiser-bessel
Ni(acac) ₂ ·2H ₂ O	Ni-O	2.549~12.161	kaiser-bessel	1.044~1.941	kaiser-bessel

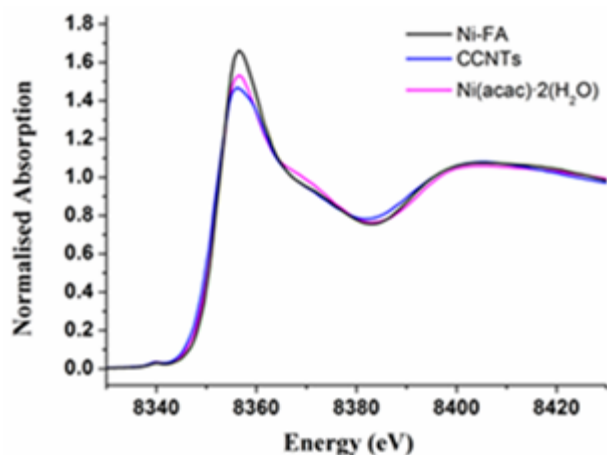


Fig. 3S Ni K-edge XANES spectra of Ni-FA, CCNTs and Ni(acac)₂·2H₂O (acac: acetylacetonate).

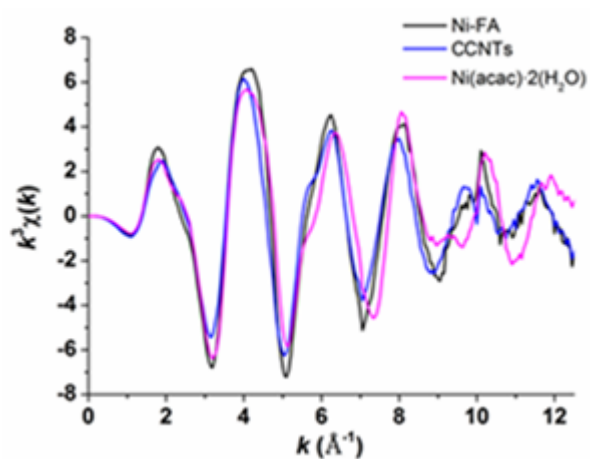


Fig. 4S Ni K-edge k³-weight EXAFS signals of Ni-FA, CCNTs and Ni(acac)₂·2H₂O.

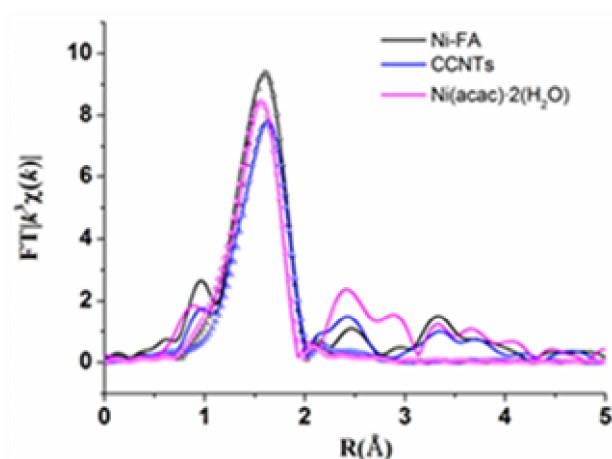


Fig. 5S Fourier transformed space (R space) and their fitting curves (dotted lines) at Ni K-edge.